Calculating the Distance to Messier 31 Using a Cepheid Variable

Scotia Rollins & Elliot Schweitzer

Pitzer College & Pomona College Department of Physics & Astronomy

December 14, 2023

Abstract

In this paper we present a modern determination of the distance to the M31 galaxy, using the method performed by Hubble in his observations 100 years prior. The Cepheid M31-V1 was observed over 49 days in October and November 2023. We performed aperture photometry on the data to produce a light curve, exposing the period of the Cepheid's change in brightness. With this period, we applied the Leavitt Law and the distance modulus to determine the distance to the star. We determined the Cepheid to have a period of 24 days, with an uncertainty of 7 days, and for it to be at a distance of 2,367,000 light years from Earth. This result agrees within 6.6% with the accepted value of 2,537,000 light years [1].

1. Background & Motivation

In 1923, a Cepheid by the name M31-V1 was discovered in the Messier 31 galaxy by Edwin Hubble. This discovery led to a shift in astronomy, due to the huge implications it had for the size of the Universe. Cepheid variable stars exhibit a unique feature that makes them objects of incredible use to astronomers: by a simple relation between their period and absolute magnitude, their distance can be determined. Hubble determined M31-V1 to be at a distance of roughly 900,000 light years from Earth, making it significantly outside the Milky Way, which at the time was estimated to have a diameter of around 300,000 light years, as opposed to the currently accepted value of 100,000 light years. We now know the distance of M31 to be closer to 2,500,000 light years. The discovery of this distant object marks the beginning of an era of major developments in observational astrophysics, and its centennial anniversary is representative of the adolescence of the fields of cosmology and extra-galactic astrophysics. For these reasons, it was our aim to recreate the discovery of M31-V1's period of variability to obtain a distance to the galaxy M31.

The relationship between a star's apparent magnitude and the period of its luminosity fluctuation was discovered by Henrietta Swan-Leavitt, from her study of Cepheids in the Large and Small Magellanic Clouds. Harlow Shapely then determine the zero point calibration required to relate the period to luminosity and absolute magnitude, allowing for a calculation of the absolute distance to the object by use of the distance modulus relation. This method was employed by Hubble in his determination of the distance to M31.

In this paper, we present our observations, photometry, and analysis of M31-V1, in an attempt to re-determine its distance by use of the Leavitt Law. To do this, we obtained images of M31-V1 over the course of a month and a half utilising the 40-inch telescope at the Table Mountain Observatory of JPL and Pomona College. Hubble's observations occurred over a period of 19 years, and he used the 100-inch telescope at Mt. Wilson Observatory. These differences yield to the fact that we new prior to the fact that M31-V1 was a Cepheid variable star with a period of around 31 days.

[1] Pommier, Rod (2022). See: https://www.astronomy.com/science/the-star-that-changed-the-cosmos-m31-v1/

Name	RA	DEC	Period (days)	V (mag)
M31-V1	00:41:27.3	+41:10:06	31.4	19.4

Table 1: Information regarding the coordinates, period and magnitude of the Cepheid.

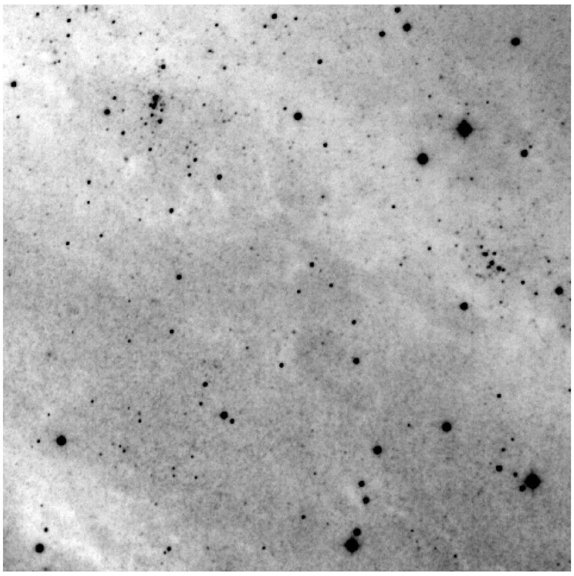

Figure 1: A photograph of our field with colour inversion, taken under the clear filter on October 19, 2023. M31-V1 lies in the center of the field.

2. Observations

With a magnitude of around 19.4, M31-V1 is a possible yet dim target for our telescope and modern CCD camera. With the prior knowledge of the Cepheid's 31 day period, we intended to record data over the span of a month and a half. We began observations on October 10th and finished on November 28th in 2023. Our final data set consisted of 16 data points within this period, as our observing possibility was subjected to weather and technical conditions. We performed observations in 3 filters; clear, g and i. In each filter, we used a 10s exposure time and took 180 frames. In our analysis, we only utilized the data taken under the clear filter.

3. Data Processing

The goal of our imaging and data reduction process was to obtain precise and accurate photometric measurements to produce a light curve with a distinct period for M31-V1. This involved calibration and stacking procedures to improve the signal-to-noise ratio, performing FWHM analysis to determine an optimal aperture size, and down selecting our targets to minimize contamination due to overlapping apertures.

3.1 Signal-to-Noise Calculation

Before photometry, we needed to ensure that our images were of high enough quality, i.e., that the ratio between the signal of the stellar sources and the noise produced by the CCD detector was as high as possible, so that the error from the noise would be minimal. To do this, we subtracted Bias frames of the CCD's inherent read-out noise, and Dark and Flat frames to reduce noise due to heat visual imperfections in the camera. Finally, rather than processing every frame individually, we combined the frames from each night into combined images.

To estimate this ratio, we applied the logic that in the limit of large N_T, the total number of electrons recorded, the Poisson distribution is well approximated by a Gaussian distribution with a standard deviation of $\sqrt{N_T}$. Thus, the signal-to-noise ratio can be approximated as:

$$\frac{S}{N} = \frac{N_T}{\sqrt{N_T}} \tag{1}$$

We estimated N_T by multiplying the electron count of M31-V1 at half of its maximum value by the area of the star in pixels. This resulted in a signal-to-noise ratio of 55. With the noise contributing to $1/55$ of the signal, the size of the error bars in the signal were 1.8% which is sufficiently small to proceed with aperture photometry. [3]

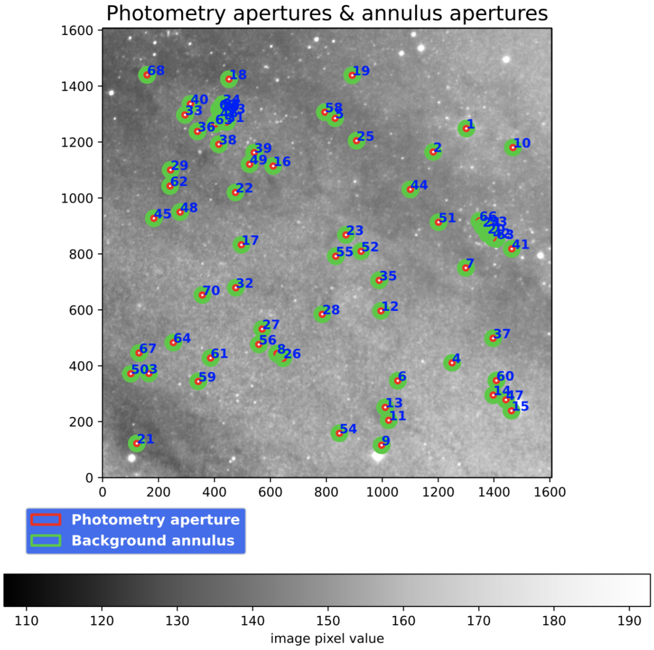

Figure 2: An image of the field taken in the clear filter, displaying the annulus apertures for the 70 brightest stars. M31-V2 is the 55th brightest star. The green annuli represent background flux, while the red annuli are the photometry apertures.

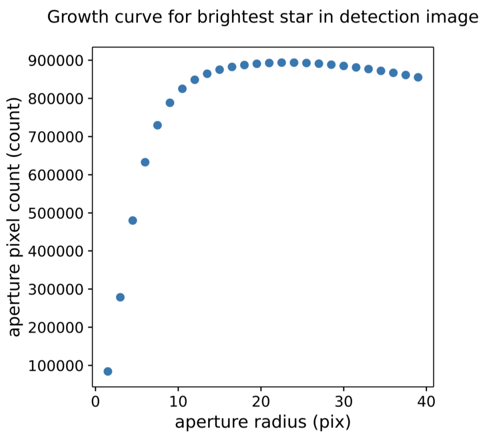

Figure 3: A growth curve of our apertures. The X-axis depecits the size of the aperture radius in pixels and the Y-axis depicts the aperture pixel count. A maximum flux is obtained around 20px, and there is turnover around 25px. The growth curve loses linearity around 7.5px radius, in accordance with our choice in aperture size.

3.2 Aperture Photometry

In order to obtain accurate photometric measurements, we performed aperture photometry in which the background flux was subtracted from the flux of the star. This can be seen in **Figure 2** where the green annuli represent the background flux and the red annuli represent the flux of the star.

To determine the radius to use for our apertures, we produced a growth curve (**Figure 3**) demonstrating the amount of flux captured over various aperture sizes. With the aim of capturing as much flux

[3]See: http://homepage.physics.uiowa.edu/ haifu//assets/pdf/astrolab/6.snr.pdf

as possible while minimizing contamination due to nearby stars, we opted to use an aperture radius of 7.5 pixels, or 2.5 in units of half width half max. The growth curve illustrates a maximum pixel count corresponding to an aperture radius of around 20 pixels, however, upon comparing light curves with different aperture radii, we discovered that a smaller aperture size resulted in less scattering. This is indicative of flux contamination due to neighbouring stars, which we also addressed by excluding such clusters in a down selection process.

3.3 FWHM Analysis

To optimize our photometry, we also performed full width half max analysis, in which we discovered a large discrepancy over the course of our observation period. This indicated an irregular spread of the measured flux of a star on different days. Using the python package imexam, which provides in depth FWHM analysis, we determined a range of 8.07px in our FWHM values– from 5.85px to 13.92px– with no trend. In order to address this, we tried separating our data into two groups of similar FWHM values based on the standard deviation, and performing photometry separately. This method did not yield any improvement in the scattering of our light curves. Our next solution involved eliminating conspicuous anomalies, which we determined to be the two nights with the highest FWHM values of 13.92 and 12.29. After this, we used a FWHM value of 6px, which was our initial visually determined value. With this, we saw improvement in the scattering of the differential magnitudes.

3.4 Down Selection & Light Curve Plotting

After the first round of differential photometry, we encountered significant scattering in the dimmer targets, which can be seen in the rightmost image in **Figure 5**. This scattering occludes the period of M31-V1 since we cannot clearly discern a difference between the Cepheid and the other stars. To address this, we decided to eliminate clusters of stars or stars whose apertures were overlapping to minimise the possibility of contamination.

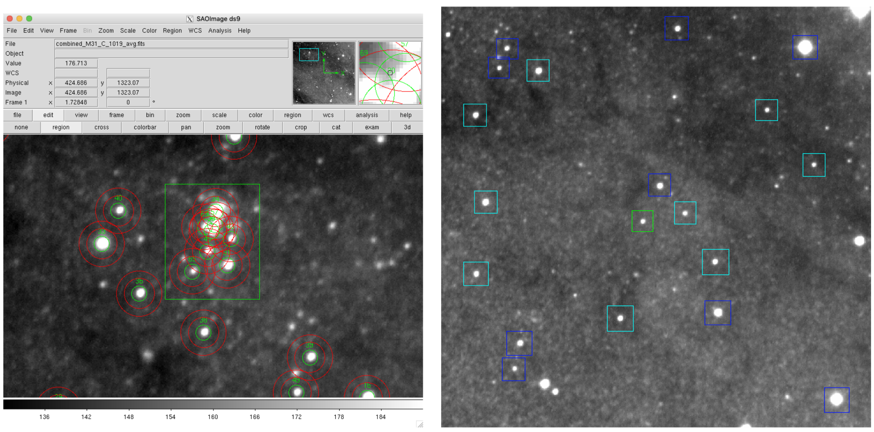

Figure 4: The left image shows a close inspection in DS9 of the overlapping of aperture annuli for close neighbouring stars. These clusters were eliminated from the data set to reduce error due to flux contamination. The right image shows our final selection of stars, chosen on the basis of their individuality and brightness.

When comparing various reference stars in observing the effect on scattering, we found that there were two main influential factors. Stars that had proximity to M31-V1 yielded less scattering. Likewise, a moderate brightness, i.e., not the dimmest and not the brightest, also provided improvement in the scattering. Thus, we concluded that the 23rd brightest star was the optimal reference star, as can be seen in **Figure 6**, with comparison to other candidates.

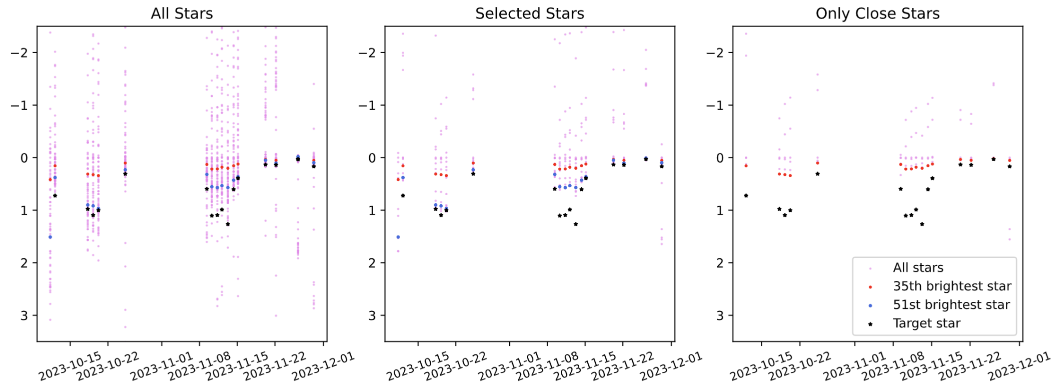

Figure 5: A comparison of the initial light curves made by all stars, then by excluding stars with nearby neighbours, then by displaying only stars close to M31-V1, from left to right. Here, the 23rd brightest star is used as a reference star. The X-axis represents the date and the Y-axis represents the differential magnitude of the stars. Between the left and middle plots, it is evident that scattering is reduced when we are more conservative with our choice in stars.

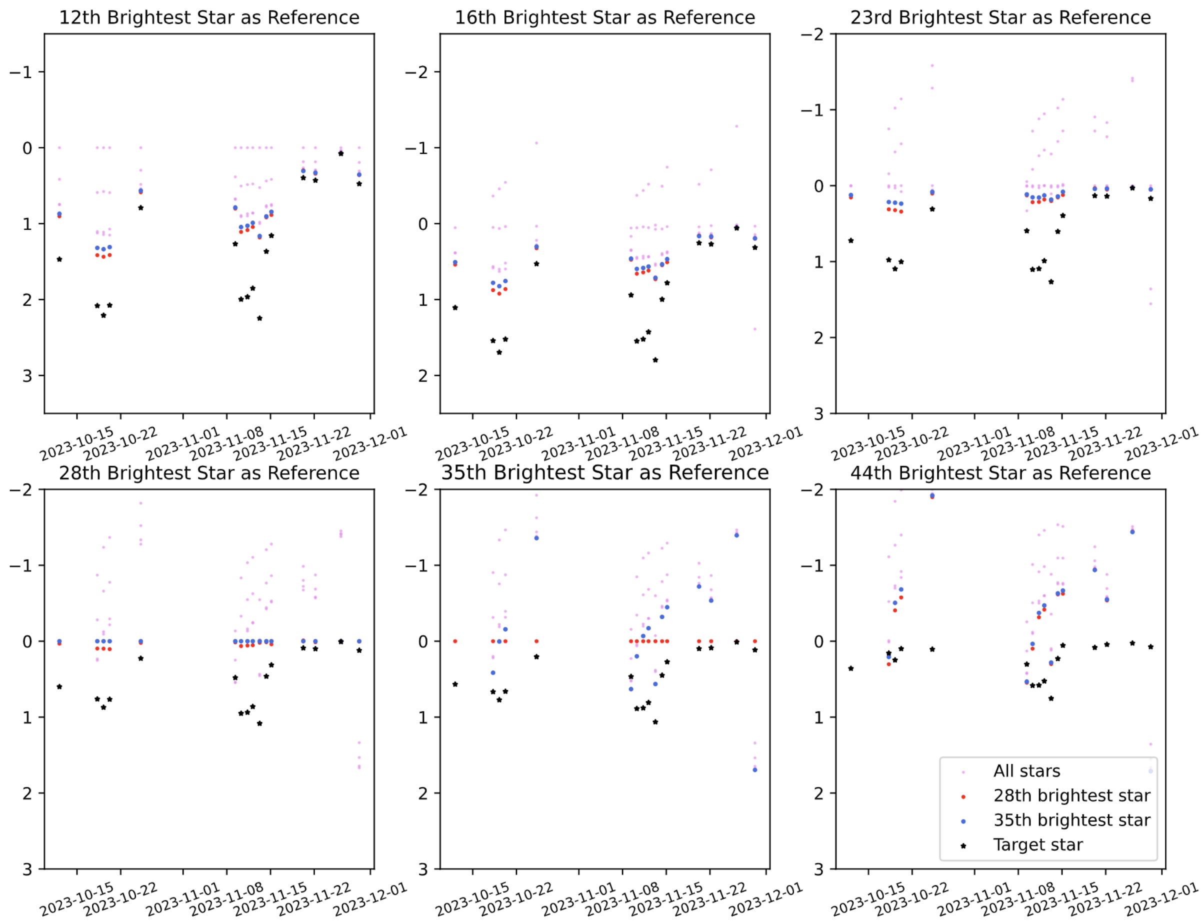

Figure 6: A comparison of the differential magnitudes with various reference stars. The X-axes represent the date and the Y-axes represent the differential magnitude of the stars. The black points show M31-V1, with the suggested trough of its period highlighted in green. The red points represent the 28th brightest star, the blue points represent the 35th brightest star, and the pink points show the rest of the stars. We discovered that the amount of scattering can be reduced by using a star that is close to M31-V1 with a moderate brightness with respect to it. Hence, the 23rd brightest star was our choice for the best reference star.

4. Data Analysis

4.1 Determining the Period

Using the 23rd brightest star as a reference, and having eliminated stars with contaminated apertures and data points with anomalous FWHM values, we significantly reduced scattering in our plot of the differential magnitudes, resulting in our final light curve (**Figure 7**). While scattering is still manifest, the fluctuation in our target's magnitude is much more distinct, allowing for the possibility of determining a period, in spite of the missing data points. We determined a period of 24 days from 2 key characteristics of the light curve.

It appears as though there are two visible troughs, the first between 10/15 and 10/22 and the second between 11/08 and 11/15. Due to the large gap in the data points, we cannot conclude that either of these ranges exhibits the actual minimum of the light curve. However, by making the assumption that these two points do exhibit local minima, they would correspond to one full period for M31-V1. In this case the minima would occur on October 19 and November 11, which are the 3rd and 8th data points from the left respectively– This corresponds to a period of 24 days.

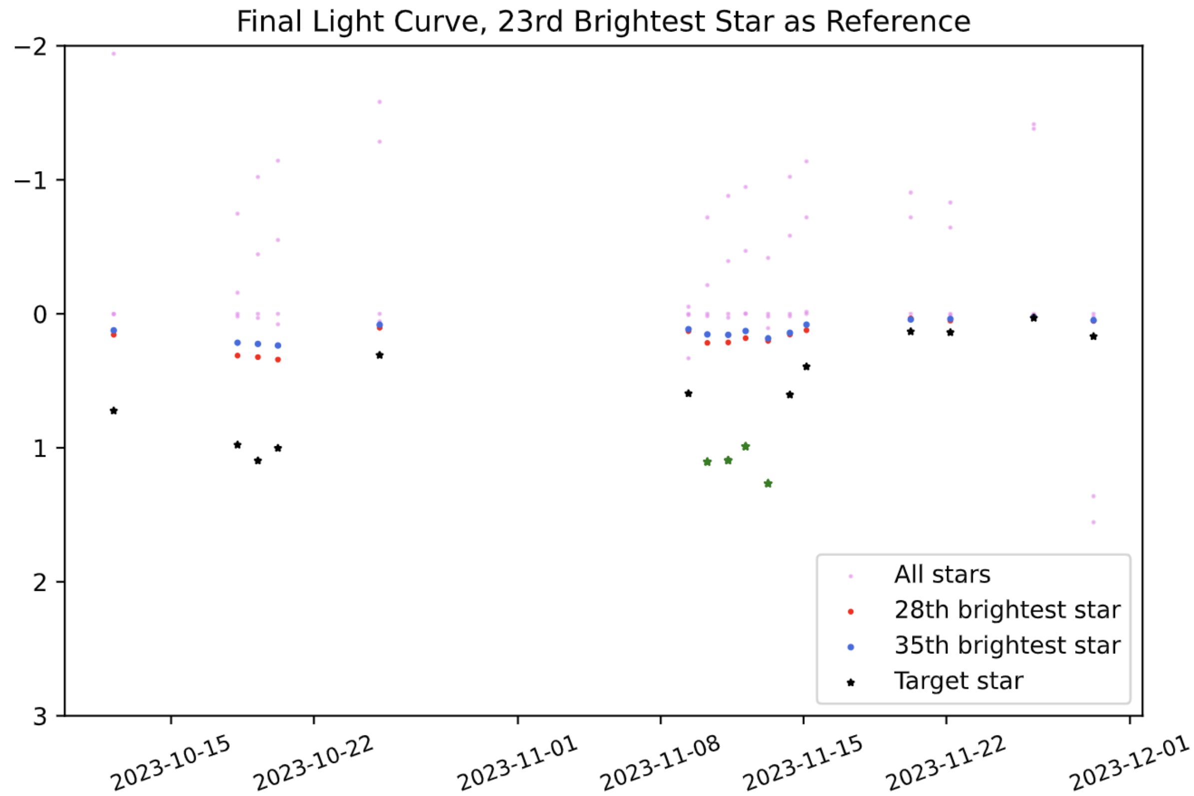

Figure 7: Our final light curve, after down selecting our targets and choosing an optimal reference star. Here, the 23rd star is the reference star. The X-axis represents the date and the Y-axis represents the differential magnitude of the stars. The black points show M31-V1, with the trough of its period highlighted in green. The red points represent the 28th brightest star, the blue points represent the 35th brightest star, and the pink points show the rest of the stars.

Alternatively, we can visualise the period by considering the appearance of a sinusoidal shape between 11/08 and 12/01. Similarly, we cannot conclude on that the points on the left of this segment exhibit the period's true minimum, but given the sinusoidal shape, and the semblance of a local maximum around 11/28, we can obtain a justifiable value for the period. Under these considerations, we take 11/10 to be a minimum and 11/22 to be a maximum. This corresponds to a half-period of 12 days, and a full period of 24 days, in accordance with the previous argument.

We should also note that the shape of a Cepheid's light curve is typically not symmetric about the minimum or maximum. Rather, the flux tends to increase at a higher rate than it decreases in every fluctuation, so the shape is not expected to be perfectly sinusoidal. Thus, for our purposes, recognising one full period in the appearance of two minima is likely more reliable– Nevertheless, the second method yields the same result.

4.2 Calculating the Distance

To calculate the distance to M31-V1 from our determination of a 24 day period, we employed the Leavitt Law which relates the period of a Cepheid to its luminosity or absolute magnitude. We also calculated an apparent magnitude, and then used the distance modulus to obtain a distance.

In order to find the apparent magnitude, we applied a zero point correction by comparing our measured value of a star's magnitude to its known value. From the catalog GSC 2.3 in DS9, we found the known V mag for our 16th brightest star to be 18 mag, while our measured value for it was 13.999. This corresponds to a zero point correction of 4 mag. The median value of the magnitude of M31-V1 between 10/11 and 11/13 was 15.33 mag. Applying the zero point correction, this corresponds to an apparent magnitude of 19.33 mag, which is in accordance with its accepted apparent magnitude of 19.4 mag.

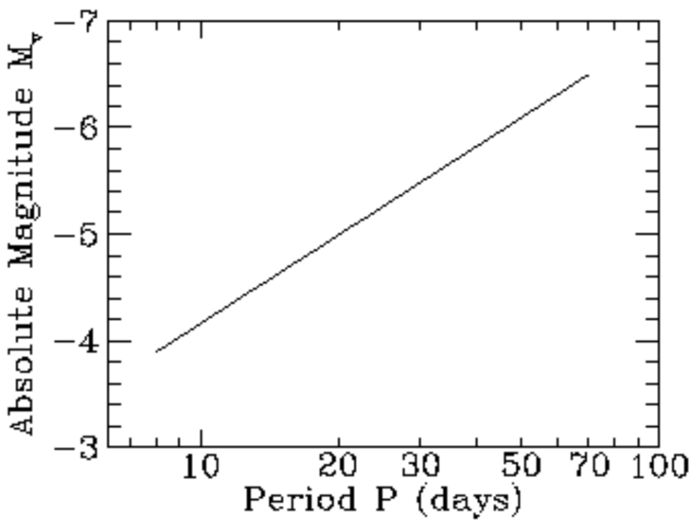

Figure 8: A plot depicting the relation between a Cepheid's period and absolute magnitude. Source: Western Kentucky University

From the period and absolute magnitude relation seen in **Figure 8**, we see that a period of 24 days corresponds to an absolute magnitude of -5.2 mag. For a more precise determination, we utilised the following relation established from Hubble Space Telescope parallaxes for nearby Cepheids[2]:

$$M_v = (-2.43 \pm 0.12)(log_{10}P - 1) - (4.05 \pm 0.02)$$

This relationship yields an absolute magnitude of -4.97 for our star. We will proceed with this value, and attribute an uncertainty of ± 0.23 mag due to the discrepancy between the methods. We can now use the distance modulus to determine the distance too M31-V1:

$$m - M = 5log_{10}(d/10pc)$$

$$10^{\frac{19.33+4.97}{5}} = d/10pc$$

$$d = 725742pc = \mathbf{2{,}367{,}000\ ly}$$

[2]Fritz Benedict, G. (2008). See: https://arxiv.org/pdf/astro-ph/0612465.pdf

4.3 Results

From the distance modulus relation, we discover a distance to M31-V1 of 2,367,000 light years. The currently accepted distance to M31-V1 is 2,537,000 light years (Pommier 2022), meaning our result is within 6.7% of the accepted value. Utilising the graph's value of -5.2mag for the absolute magnitude yields a distance of 2,620,000 light years for M31-V1, which is closer to the accepted value. However, this method yields greater uncertainty due to the imprecision of the visual estimation of the value. Moreover, our value for 24 days of the period, which is less than the accepted 31 days, would imply an underestimate for the value of the distance, not an over estimate. For this reason, we adhere with the empirical relation determined using HST in 2008. **Table 2** displays all our results.

Instrumental Magnitude	Apparent Magnitude	Absolute Magnitude	Distance (ly)	Distance (pc)
15.33 mag	19.33 mag	-4.97 mag	2,367,000	725742

Table 2: The result of our observations and analysis. The columns shows the instrumental magnitude, the apparent magnitude, the absolute magnitude and the distance to M31-V1.

4.4 Error & Uncertainty

The uncertainty in our results can be attributed to several factors, including the calibration from instrumental to apparent magnitude, aperture inefficiency, and errors inherent to the equipment that were unaccounted for in the subtraction of calibration frames. Finally, we must account for error due to the missing data points and the visual determination of the period– The preceding factors are expected to be trivial compared to this. We expect the error from the calibration of the apparent magnitude to be small since we performed a direct comparison between known values and obtained values for a star in our field. The inconsistency in the FWHM across nights is a source of uncertainty, however, this is unlikely to have a significant effect on the shape of the light curve and our determination of the period. It may however, be the cause of the scattering in the differential magnitudes. From this, we attribute an uncertainty of 0.25mag to the differential magnitudes, accounting for aperture inefficiency, FWHM inconsistency, and internal errors.

Our light curve exhibits a significant gap of missing data points between 10/25 and 11/09, making it impossible to know where the peak lies between these dates. For this, we estimate an uncertainty of 7 days to the period, which is half of this unknown gap. The upper limit for our period is then 31 days, which is the period determined by Hubble in the star's original discovery. This corresponds to a 11.5% uncertainty in the distance. However, because our result is within 6.6% of the accepted value, we can be confident that the actual error is smaller than this.

5. Discussion & Conclusion

Our objective in this project was to recreate Hubble's measurement of the period of the Cepheid M31-V1 to determine the distance to M31. We found a distance for the star of 2,367,000 light years, and a period for it of 24 days. The data for this project were obtained over a 49 day period, and the images were processed using aperture photometry to obtain a light curve of differential magnitudes. From this, we applied the period-luminosity relation and the distance modulus to obtain our result. Our findings adhere with the modern value of the distance to M31 within an acceptable range, given the short term nature of this project.

5.1 Acknowledgments

We thank Professor Philip Choi for his guidance and advice, and Nez Evans for obtaining the data. Additionally, thanks to Nadia Shwartz Bolef, Auggie Davis, Lauren Mae Henson, Jacob Kianovsky, Abby Tiller, Braden Bouwman, Isa Hahn, Sage Santomenna and Inq Soncharoen for their contributions.

References

Fritz Benedict, G. (2008). *Hubble Space Telescope Fine Guidance Sensor Parallaxes of Galactic Cepheid Variable Stars: Period-Luminosity Relations.*
Retrieved from: https://arxiv.org/pdf/astro-ph/0612465.pdf

Hubble, Edwin (1923). *A Sprial Nebula as a Stellar System, Messier 31.*
American Astronomical Society, Washington, DC

Pommier, Rod (2022). *The Star that Changed the Cosmos: M31-V1.*
Retrieved from: https://www.astronomy.com/science/the-star-that-changed-the-cosmos-m31-v1/

Templeton, M. (2011). *Modern Observations of Hubble's First Discovered Cepheid in M31.*
Retrieved from: https://www.jstor.org/stable/10.1086/663651

University of Iowa. *Signal to Noise Ratio.*
Retrieved from: http://homepage.physics.uiowa.edu/ haifu//assets/pdf/astrolab/6.snr.pdf

Western Kentucky University. *The Period Luminosity Relation.*
Retrieved from: http://astro.wku.edu/labs/m100/PLrelation.html: :text=Cepheids